

**This is an electronic reprint of the original article.
This reprint *may differ* from the original in pagination and typographic detail.**

Author(s): Anjam, Immanuel; Mali, Olli; Neittaanmäki, Pekka; Repin, Sergey

Title: New Indicators of Approximation Errors for Problems in Continuum Mechanics

Year: 2010

Version:

Please cite the original version:

Anjam, I., Mali, O., Neittaanmäki, P., & Repin, S. (2010). New Indicators of Approximation Errors for Problems in Continuum Mechanics. In J. C. F. Pereira, A. Sequeira, & J. M. C. Pereira (Eds.), Proceedings of the Fifth European Conference on Computational Fluid Dynamics ECCOMAS CFD 2010 (CD-ROM).

All material supplied via JYX is protected by copyright and other intellectual property rights, and duplication or sale of all or part of any of the repository collections is not permitted, except that material may be duplicated by you for your research use or educational purposes in electronic or print form. You must obtain permission for any other use. Electronic or print copies may not be offered, whether for sale or otherwise to anyone who is not an authorised user.

NEW INDICATORS OF APPROXIMATION ERRORS FOR PROBLEMS IN CONTINUUM MECHANICS

Immanuel B. Anjam¹, Olli J. Mali²,
Pekka J. Neittaanmäki³ and Sergey I. Repin⁴

^{1,2,3}University of Jyväskylä,
Department of Mathematical Information Technology,
P.O. Box 35 (Agora), FI-40014 University of Jyväskylä, Finland
e-mail: {immanuel.anjam, olli.mali, pn}@jyu.fi

⁴V. A. Steklov Institute of Mathematics in St. Petersburg
Fontanka 27, RU-191024, St. Petersburg, Russia
e-mail: repin@pdmi.ras.ru

Key words: continuum mechanics, a posteriori, error indicator, reliable numerical methods

Abstract. *In this paper we present a new error indicator for approximate solutions of elliptic problems. We discuss error indication with the paradigm of the diffusion problem, however the techniques are easily adaptable to more complicated elliptic problems, for example to linear elasticity, viscous flow models and electromagnetic models. The proposed indicator does not contain mesh dependent constants and it admits parallelization.*

1 INTRODUCTION

Various a posteriori indicators of approximation errors are widely used in computer simulation. Error indicators for finite element approximations are usually based either on evaluation of a weak residual norm or on post-processing (e.g., gradient averaging) and are applicable only to Galerkin approximations. In this paper, we discuss a different class of error indicators that follow from a posteriori estimates of the functional type (a consequent exposition of the corresponding theory is given in the books^{5,7}). These estimates do not contain mesh dependent constants, do not exploit specific properties of the numerical method or approximations used and are valid for any conforming approximation.

In this paper, we modify some ideas of the functional approach and derive error indicators of a new type. The indicators contain the corresponding numerical solution v , problem data and an arbitrary function y , which is to be selected in a suitable way. For this task, we apply two different methods (global and local) and compare their efficiency.

Let Ω be a bounded and connected domain in \mathbb{R}^d with Lipschitz boundary $\partial\Omega$. Consider the the following problem: find a scalar function u such that

$$-\operatorname{div} \mathbf{A} \nabla u = f \quad \text{in } \Omega, \quad (1)$$

$$u = 0 \quad \text{on } \partial\Omega, \quad (2)$$

where \mathbf{A} is a symmetric $d \times d$ matrix with coefficients in $L^\infty(\Omega)$ and $f \in L^2(\Omega)$. The generalized solution to this problem is a function $u \in \mathring{H}^1(\Omega)$ that satisfies the relation

$$\int_{\Omega} \mathbf{A} \nabla u \cdot \nabla w \, dx = \int_{\Omega} f w \, dx, \quad \forall w \in \mathring{H}^1(\Omega), \quad (3)$$

where $\mathring{H}^1(\Omega)$ is the space of functions from $H^1(\Omega)$ which vanish on $\partial\Omega$. For this problem the natural energy norm is defined as

$$\| u \|^2 := \|\nabla u\|_{\mathbf{A}}^2 := \int_{\Omega} \mathbf{A} \nabla u \cdot \nabla u \, dx.$$

We denote by $\| \cdot \|$ the L_2 norm of scalar- and vector-valued functions.

2 ERROR MAJORANT AND INDICATOR

Guaranteed error bounds for the problem (1)-(2) are derived by transformations of the integral identity (3), which lead to the following result^{5,7}.

Proposition 2.1. *Let u be the exact solution and $v \in \mathring{H}^1(\Omega)$ a numerical solution to the problem (1)-(2). Then*

$$\| u - v \| \leq M_{\oplus}(v, y), \quad \forall y \in H(\operatorname{div}, \Omega),$$

where

$$M_{\oplus}(v, y) := C_{\Omega} \|f + \operatorname{div} y\| + \|y - \mathbf{A}\nabla v\|_{\mathbf{A}^{-1}}. \quad (4)$$

Here C_{Ω} is the constant in the Friedrichs inequality and $y \in H(\operatorname{div}, \Omega)$ is an arbitrary function.

The quality of the majorant (4) depends on how well the arbitrary function y represents the exact flux $p = \mathbf{A}\nabla u$. This estimate does not contain a gap between the exact error and the estimate. This fact is easy to establish by replacing y with the exact flux. The first term vanishes and the majorant becomes

$$M_{\oplus}(v, p) = \|\nabla(u - v)\|_{\mathbf{A}} = \|u - v\|.$$

Indeed, if the free function y is chosen properly, the first term of majorant (4) is small. Therefore it is reasonable to assume that we can define the following error indicator from the latter term of the majorant.

Proposition 2.2. *Let u be the exact solution and $v \in \mathring{H}^1(\Omega)$ a numerical solution to the problem (1)-(2). We define the error indicator*

$$I(v, y) := \|y - \mathbf{A}\nabla v\|^2, \quad (5)$$

where $y \in H(\operatorname{div}, \Omega)$ is an arbitrary function. The indicator I estimates the distribution of $\|u - v\|^2$ in the domain Ω .

3 OBTAINING THE ARBITRARY FUNCTION y

The majorant and the indicator contain the arbitrary function y , which we call the flux. In this section we show several ways how to obtain this parameter for the diffusion problem. These same methods can be used also for other elliptic problems.

The problem of finding y for the diffusion problem burns down to approximating the exact flux $p = \mathbf{A}\nabla u$. There are several ways to obtain estimates to the exact flux. First we discuss the global minimization technique, and then we propose a (new) local minimization procedure.

3.1 Global minimization

One way to obtain good approximations for the exact flux is to minimize the majorant M_{\oplus} defined by (4) globally with respect to y . For this we transform the majorant to a quadratic form. This is done by squaring the majorant and using the algebraic inequality $(a + b)^2 \leq (1 + \beta)a^2 + (1 + \frac{1}{\beta})b^2$ which holds for all $\beta > 0$. The estimate proposed in 2.1 becomes

$$\|u - v\|^2 \leq \mathcal{M}(v, y, \beta) := (1 + \beta)C_{\Omega}^2 \|f + \operatorname{div} y\|^2 + \left(1 + \frac{1}{\beta}\right) \|y - \mathbf{A}\nabla v\|_{\mathbf{A}^{-1}}^2. \quad (6)$$

Minimizing (6) globally results in the following finite element problem for $y \in H(\operatorname{div}, \Omega)$:

$$\begin{aligned} (1 + \beta)C_\Omega^2 \int_\Omega \operatorname{div} y \operatorname{div} \phi \, dx + \left(1 + \frac{1}{\beta}\right) \int_\Omega \mathbf{A}^{-1} y \cdot \phi \, dx = \\ = -(1 + \beta)C_\Omega^2 \int_\Omega f \operatorname{div} \phi \, dx + \left(1 + \frac{1}{\beta}\right) \int_\Omega \phi \cdot \nabla v \, dx. \quad \forall \phi \in H(\operatorname{div}, \Omega). \end{aligned}$$

A natural choice to solve this problem is to use Raviart-Thomas elements^{4,6}. This method produces good approximations for the exact flux, but is relatively time-consuming. For error indication purposes less expensive methods are preferable.

3.2 Averaging procedures

A very popular method to approximate the exact flux is to post-process the approximate flux $\mathbf{A}\nabla v$ ^{1,3,8}. If v belongs to the space $H^1(\Omega)$, then its gradient ∇v is constant in each element. If also the matrix \mathbf{A} is constant in each element, we can apply very simple averaging procedures to the approximate flux.

A common way is to average the approximate flux to nodes: for each node, calculate $\mathbf{A}\nabla v$ in each related element and average the values weighted by the areas of respective elements. We denote this procedure by G_N .

It is also possible to average the normal components of the approximate flux. In 2D these values are averaged to edges of elements. Let c_{nl} denote the unknown degree of freedom related to edge e_{nl} with edge length $|e_{nl}|$. Here the subindex letters n and l denote the numbers of the nodes which define the edge. We denote by T_{knl}, T_{nml} the elements related to this edge and by n_{knl}, n_{nml} their respective unit outward normals on the boundary. This setting is visualized in Figure 1. The following equation averages the normal component of $\mathbf{A}\nabla v$ to the edge e_{nl} :

$$c_{nl} = \frac{|e_{nl}| (\mathbf{A}\nabla v|_{T_{knl}} \cdot n_{knl} - \mathbf{A}\nabla v|_{T_{nml}} \cdot n_{nml})}{2} \quad (7)$$

In 3D the normal components are averaged in a similar way. The only difference is that now we average the values to faces instead of edges. Let c_{nlm} denote the unknown degree of freedom related to face f_{nlm} whose area is $|f_{nlm}|$. We denote by T_{knlm}, T_{omln} the elements related to this face and by n_{knlm}, n_{omln} their respective unit outward normals on the boundary, see Figure 1. The following equation averages the normal component of $\mathbf{A}\nabla v$ to the face f_{nlm} :

$$c_{nlm} = \frac{|f_{nlm}| (\mathbf{A}\nabla v|_{T_{knlm}} \cdot n_{knlm} - \mathbf{A}\nabla v|_{T_{omln}} \cdot n_{omln})}{2} \quad (8)$$

We denote by G_{RT} the procedure, which calculates the values of (7) for all edges or (8) for all faces in a given mesh. It should be noted that the operator G_{RT} essentially produces functions from linear Raviart-Thomas finite element space.

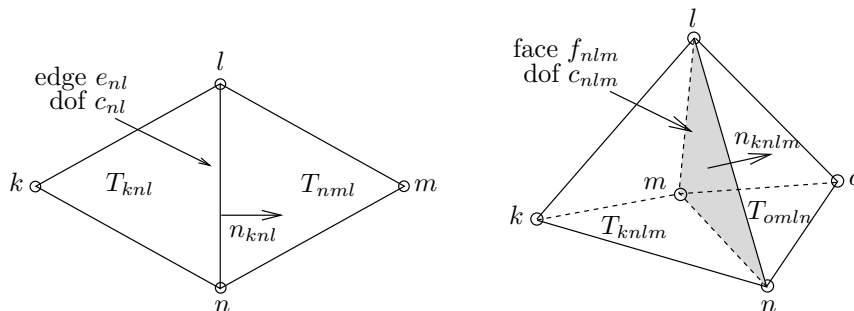


Figure 1: Two neighboring elements in 2D and 3D.

3.3 A post-processing method

In this section we present a post-processing method which gives even better approximations for the exact flux $\mathbf{A}\nabla u$. Assume that the initial approximation is obtained by the averaging operator G_{RT} defined in the previous section. In our previous paper² we made further post-processing of the approximate flux (for the poisson problem) by minimizing only a part of the majorant. In this paper we take this same idea further and choose to post-process $y = G_{RT}(\mathbf{A}\nabla v)$ by minimizing the whole majorant \mathcal{M}_{\oplus} on every pair of neighboring triangular elements. Next we show how to do this in 3D (the 2D case is very similar).

Since y is computed by the averaging operator G_{RT} , it can be represented as

$$y = \sum_{\alpha=1}^{NF} c_{\alpha} \phi_{\alpha},$$

where NF is the number of faces, c_{α} are the degrees of freedom computed by G_{RT} , and ϕ_{α} are the global basis functions for linear Raviart-Thomas finite element space. To conveniently mark local basis functions related to two particular elements (see Figure 1) we introduce the index-sets

$$\begin{aligned} \mathbb{I}_1 &= \{nlm, mlk, kln, nmk\}, & \text{indices to faces of element } T_{knlm}, \\ \mathbb{I}_2 &= \{mln, nlo, olm, mno\}, & \text{indices to faces of element } T_{omln}. \end{aligned}$$

Our goal is to minimize the quantity

$$\mathcal{J}(y) := \int_{T_{knlm} \cup T_{omln}} (C(f + \operatorname{div} y)^2 + (y - \mathbf{A}\nabla v) \cdot (\mathbf{A}^{-1}y - \nabla v)) dx$$

by optimizing the degree of freedom c_{nlm} ($= c_{mln}$) shared by the two elements. Here

$C = (1 + \beta)C_\Omega(1 + \frac{1}{\beta})^{-1}$. This one-parametric problem is easily solved:

$$\begin{aligned} \frac{\partial \mathcal{J}}{\partial c_{nlm}} &= 2 \int_{T_{knlm}} \left(C \left(f + \sum_{\alpha \in \mathbb{I}_1} c_\alpha \operatorname{div} \phi_\alpha \right) \operatorname{div} \phi_{nlm} - \phi_{nlm} \cdot \nabla v + \sum_{\alpha \in \mathbb{I}_1} c_\alpha \phi_\alpha \cdot \mathbf{A}^{-1} \phi_{nlm} \right) dx + \\ &+ 2 \int_{T_{omln}} \left(C \left(f + \sum_{\alpha \in \mathbb{I}_2} c_\alpha \operatorname{div} \phi_\alpha \right) \operatorname{div} \phi_{mln} - \phi_{mln} \cdot \nabla v + \sum_{\alpha \in \mathbb{I}_2} c_\alpha \phi_\alpha \cdot \mathbf{A}^{-1} \phi_{mln} \right) dx = 0. \end{aligned}$$

From the above we can solve a new value for the degree of freedom c_{nlm} :

$$c_{nlm} = \frac{A}{B}, \quad (9)$$

where

$$\begin{aligned} A &= \\ &\int_{T_{knlm}} \left(C \left(f + \sum_{\alpha \in \mathbb{I}_1 \setminus \{nlm\}} c_\alpha \operatorname{div} \phi_\alpha \right) \operatorname{div} \phi_{nlm} - \phi_{nlm} \cdot \nabla v + \sum_{\alpha \in \mathbb{I}_1 \setminus \{nlm\}} c_\alpha \phi_\alpha \cdot \mathbf{A}^{-1} \phi_{nlm} \right) dx + \\ &+ \int_{T_{omln}} \left(C \left(f + \sum_{\alpha \in \mathbb{I}_2 \setminus \{mln\}} c_\alpha \operatorname{div} \phi_\alpha \right) \operatorname{div} \phi_{mln} - \phi_{mln} \cdot \nabla v + \sum_{\alpha \in \mathbb{I}_2 \setminus \{mln\}} c_\alpha \phi_\alpha \cdot \mathbf{A}^{-1} \phi_{mln} \right) dx, \end{aligned}$$

and

$$B = - \int_{T_{knlm}} \left(C(\operatorname{div} \phi_{nlm})^2 + \phi_{nlm} \cdot \mathbf{A}^{-1} \phi_{nlm} \right) dx - \int_{T_{omln}} \left(C(\operatorname{div} \phi_{mln})^2 + \phi_{mln} \cdot \mathbf{A}^{-1} \phi_{mln} \right) dx.$$

We denote by P the procedure, which calculates the values of (9) for all degrees of freedom in a given mesh.

It should be noted, that the operator P can be applied to y as many times as wanted, and each time the value of $\mathcal{J}(y)$ decreases. In other words, the process is *monotone*. This post-processing method is also practical since it easily adapts parallelization.

4 NUMERICAL EXAMPLES

In this section, we test the performance of the error majorant M_\oplus and indicator I with various methods of selecting y , which were derived in the previous section. For the purpose of measuring the performance of the majorant, we define the *efficiency index*

$$I_{eff} = \frac{M_\oplus}{\|u - v\|}.$$

The performance of the error indicator is tested by comparing the error distribution provided by the indicator to the exact error distribution.

To solve the model problem (1)-(2) we use the linear H^1 finite element. For the arbitrary function y we use both the post-processing operators G_N , G_{RT} , and P and the global minimization method. For global minimization, we use the linear Raviart-Thomas finite element. In all numerical examples, the arbitrary function y is computed on the same mesh on which the original numerical approximation v was computed.

Example 1:

$$\begin{aligned}\Omega &= [0, 1]^2, & f &= 2(x_1(1 - x_1) + x_2(1 - x_2)), \\ \mathbf{A} &= \{a_{11} = a_{22} = 1, a_{12} = a_{21} = 0\}.\end{aligned}$$

For this problem the exact solution is known. Table 1 shows how the integral $\mathcal{J}(y)$ and the efficiency indexes I_{eff} for the upper bound $M_{\oplus}(v, y)$ behave with different y and different mesh-sizes. Post-processing methods G_N and G_{RT} fail to produce a flux that would satisfy the equilibrium condition, $\operatorname{div} y + f = 0$. For this reason, they do not provide a very accurate upper bound, and the values of I_{eff} are relatively large. By further post-processing, the value of the efficiency index can be decreased close to the one obtained by globally solved y_{glo} . According to numerical experiments, five iteration rounds are enough independent of the mesh size.

Example 2:

$$\begin{aligned}\Omega &= [0, 1]^2, & f &= 2(10x_1(1 - x_1) + x_2(1 - x_2)), \\ \mathbf{A} &= \{a_{11} = 1, a_{22} = 10, a_{12} = a_{21} = 0\}.\end{aligned}$$

Also for this problem the exact solution is known. Figure 2 shows how the indicator I performs with different y in the second test example. Those elements, on which the error is greater than the average error, are marked with black color. In the top row, the leftmost picture is the exact error distribution. Here again y_{glo} denotes the function obtained by global minimization. As expected, global minimization of the upper bound gives good results. By using the operators G_N and G_{RT} we obtain good representations of error distributions. Moreover, further equilibration of $G_{RT}(\mathbf{A}\nabla v)$ by using the operator P does clearly improve the performance of I .

Example 3:

$$\begin{aligned}\Omega &= [0, 2]^2, \\ f &= \begin{cases} 1 & \text{for } x_1 \in (0.5, 1.5) \\ 0 & \text{otherwise} \end{cases}, \\ \mathbf{A} &= \begin{cases} \{a_{11} = 1, a_{22} = 1, a_{12} = a_{21} = 0\} & \text{for } x_1 \in (0.5, 1.5) \\ \{a_{11} = 10, a_{22} = 1, a_{12} = a_{21} = 0\} & \text{otherwise} \end{cases}.\end{aligned}$$

For this problem we do not know the exact solution. A reference solution was calculated in a very fine mesh to obtain a reference error distribution. From Figure 3 we see that this example is much more difficult compared to the previous example.

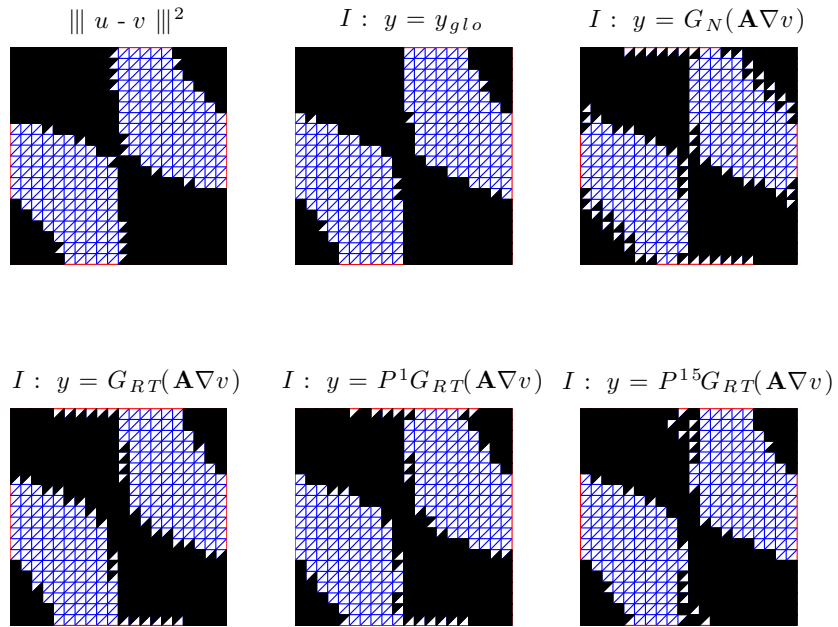


Figure 2: Performance of the post-processing operator P and the indicator I for Example 2.

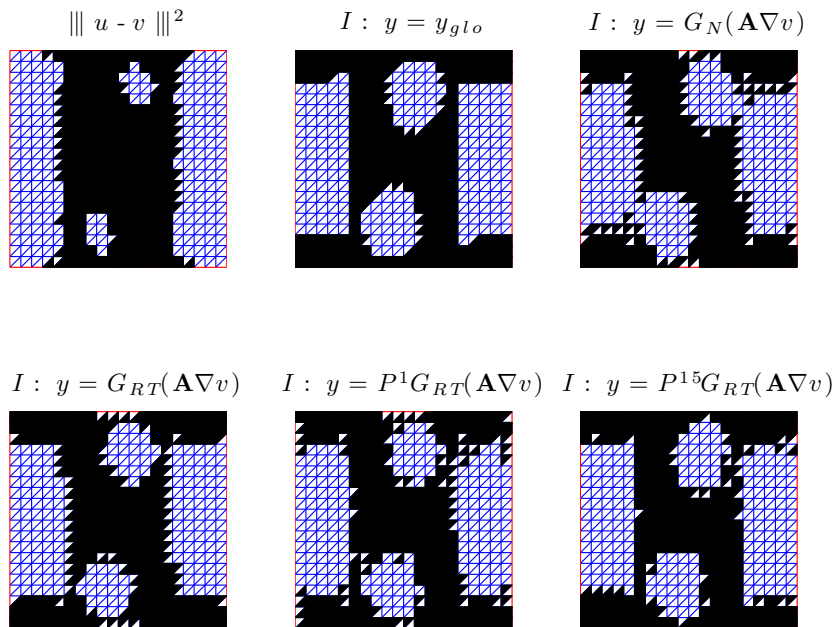


Figure 3: Performance of the post-processing operator P and the indicator I for Example 3.

	82 elems		1342 elems		8562 elems	
function y	\mathcal{J}	I_{eff}	\mathcal{J}	I_{eff}	\mathcal{J}	I_{eff}
$G_N(\mathbf{A}\nabla v)$	2.36e-3	2.46	2.48e-4	4.02	6.09e-5	6.53
$G_{RT}(\mathbf{A}\nabla v)$	3.24e-3	2.88	6.42e-4	8.35	2.00e-4	16.81
$P^1 G_{RT}(\mathbf{A}\nabla v)$	2.40e-3	2.06	3.04e-4	3.80	8.10e-5	6.59
$P^2 G_{RT}(\mathbf{A}\nabla v)$	2.17e-3	1.85	1.80e-4	2.25	3.93e-5	3.21
$P^5 G_{RT}(\mathbf{A}\nabla v)$	2.07e-3	1.77	1.44e-4	1.79	2.34e-5	1.91
y_{glo}	2.00e-3	1.75	1.34e-4	1.72	2.06e-5	1.72

 Table 1: Integral $\mathcal{J}(y)$ and efficiency index I_{eff} values with different mesh sizes and y for Example 1.

5 CONCLUSIONS

We conclude that in order to compute an efficient upper bound for the approximation error, the main problem is to obtain well enough equilibrated flux (minimizer of $\mathcal{J}(y)$). This task can be done with feasible computational effort using the presented new post-processing technique, which admits parallel processing.

For the purpose of obtaining the error distribution, the examples computed here do demonstrate some difference between the various post-processing methods tested. The averaging operators alone were able to represent the approximate flux well, but the proposed post-processing operator P was clearly shown to improve the quality of the approximate flux. As a natural consequence also the quality of error distributions was better after applying the post-processing operator P .

Acknowledgement. This research was supported by the grant N 40234 and N 40277 of the MASI Tekes Technology Programme and grant N 116895 of the Academy of Finland.

REFERENCES

- [1] M. Ainsworth and J. T. Oden, A posteriori error estimation in finite element analysis, *Wiley ans Sons*, New York, (2000).
- [2] I. Anjam, O. Mali, P. Neittaanmäki and S. Repin, A New Error Indicator for the Poisson Problem, In proceedings of the *10th Finnish Mechanics Days*, Jyväskylä, Finland, (2009).
- [3] I. Babuška and R. Rodriguez, The problem of the selection of an a posteriori error indicator based on smoothing techniques, *Internat. J. Numer. Meth. Engrg.*, **36**, 539–567, (1993).
- [4] F. Brezzi and M. Fortin, Mixed and hybrid finite element methods, *Springer Series in Computational Mathematics*, **15**, New York, (1991).
- [5] P. Neittaanmäki and S. Repin, Reliable methods for computer simulation. Error control and a posteriori estimates, *Elsevier*, Amsterdam, (2004).

- [6] P. A. Raviart and J. M. Thomas, Primal hybrid finite element methods for 2nd order elliptic equations, *Math. Comput.*, **31**, 391–413, (1977).
- [7] S. Repin, A Posteriori Estimates for Partial Differential Equations, *Walter de Gruyter*, Berlin, (2008).
- [8] O. C. Zienkiewicz and J. Z. Zhu, A simple error estimator and adaptive procedure for practical engineering analysis, *Internat. J. Numer. Meth. Engrg.*, **24**, 337–357, (1987).